Molecular Pharmacology Fast Forward. Published on July 7, 2011 as doi:10.1124/mol.111.072421

Title Page

The antiepileptic drugs Phenobarbital and Carbamazepine reduce transport of methotrexate in rat choroid plexus by downregulation of the Reduced folate carrier

Sandra Halwachs, Cathleen Lakoma, Ingo Schäfer, Peter Seibel, and Walther Honscha

Institute of Pharmacology, Pharmacy and Toxicology, Faculty of Veterinary Medicine, Universität Leipzig, Leipzig, Germany (S.H., C.L., W.H.); and Molecular Cell Therapy, Center for Biotechnology and Biomedicine, Faculty of Medicine, Universität Leipzig, Leipzig, Germany (I.S., P.S.)

Molecular Pharmacology Fast Forward. Published on July 7, 2011 as DOI: 10.1124/mol.111.072421
This article has not been copyedited and formatted. The final version may differ from this version.

Running title page

a) *Running title:* PB and CBZ cause downregulation of Rfc1 in choroid plexus

b) *Address correspondence to:* Sandra Halwachs, Institute of Pharmacology, Pharmacy and Toxicology, Faculty of Veterinary Medicine, An den Tierkliniken 15, University of Leipzig, 04103 Leipzig, Germany; Tel.: +49 (0) 341-9738142, FAX +49 (0) 341-9738149; E-mail: halwachs@vetmed.uni-leipzig.de

c) Number of text pages: 31

tables: 1

figures: 8

references: 38

Number of words: Abstract: 247

Introduction: 717

Discussion: 1364

d) *Abbreviations:* ALL, acute lymphoblastic leukemia; AEDs, antiepileptic drugs; Bcrp, breast cancer resistance protein; CAR, constitutive androstane receptor; CBZ, carbamazepine; CP, choroid plexus; BCSF barrier, blood-cerebrospinal-fluid barrier; CSF, cerebrospinal-fluid; DHFR, dihydrofolate reductase; FOLR, folate receptor; 5-MTHF, 5-methyltetrahydrofolate; MTX, methotrexate; IT, intrathecal; Mrp, multidrug resistance-associated protein; Oat, organic anion transporter; Oatp, organic anion transporting polypeptide; PAH, para-aminohippurate; PB, phenobarbital; PCFT, proton-coupled folate transporter; PKC, protein kinase C; TJP, tight junction protein; ZO-1, zonula occludens-1

Molecular Pharmacology Fast Forward. Published on July 7, 2011 as DOI: 10.1124/mol.111.072421
This article has not been copyedited and formatted. The final version may differ from this version.

Abstract

Intrathecal methotrexate (MTX) has been associated with severe neurotoxicity. As carrier-associated removal of MTX from the cerebrospinal-fluid (CSF) into blood remains undefined, we determined expression and function of MTX transporters in rat choroid plexus (CP). MTX neurotoxicity usually manifests as seizures requiring therapy with antiepileptic drugs (AEDs) like phenobarbital (PB). As we have demonstrated that PB reduces activity of MTX influx carrier Rfc1 in liver, we investigated the influence of the AEDs PB, carbamazepin (CBZ) or gabapentin on Rfc1-mediated MTX transport in CP. RT-PCR and Western blot analysis showed similar expression of the MTX influx carrier Rfc1 and Oat3 or efflux transporter Mrp1 and Bcrp in rat CP tissue and choroidal epithelial Z310 cells. Confocal microscopy revealed subcellular localization of Rfc1 and Bcrp at the apical and of Mrp1 at the basolateral CP membrane. Uptake, efflux as well as inhibition studies indicated MTX transport activity of Rfc1, Mrp1, and Bcrp. PB and CBZ but not gabapentin significantly inhibited Rfc1-mediated uptake of MTX in CP cells. Studies on the regulatory mechanism showed that PB significantly inhibited Rfc1 translation but did not alter carrier gene expression. Altogether, removal of intrathecal MTX across the blood-CSF barrier may be achieved through Rfc1-mediated uptake from the CSF followed by MTX extrusion into blood particularly via Mrp1. Antiepileptic treatment with PB or CBZ causes posttranscriptional downregulation of Rfc1 activity in CP. This mechanism may result in enhanced MTX toxicity in cancer patients receiving intrathecal MTX chemotherapy by reduced CSF clearance of the drug.

Molecular Pharmacology Fast Forward. Published on July 7, 2011 as DOI: 10.1124/mol.111.072421
This article has not been copyedited and formatted. The final version may differ from this version.

Introduction

In patients with acute lymphoblastic leukemia (ALL) or lymphoma, the folate antagonist methotrexate (MTX) is the commonest chemotherapeutic drug employed in central nervous system (CNS) prophylaxis and treatment and is associated with a reduction in CNS relapse (Kwong et al., 2009). Despite its clinical success, intrathecal (IT) MTX has been shown to involve significant neurotoxicity (Shuper et al., 2002), whose pathogenic mechanism is as yet poorly understood. The antifolate MTX mainly inhibits the enzyme DHFR resulting in inhibition of DNA synthesis and cell death through depletion of reduced folate cofactors, including 5-methyltetrahydrofolate (5-MTHF) (Shuper et al., 2002). Moreover, lack of the carbon donor 5-MTHF reduces the conversion of homocysteine to methionine resulting in hyperhomocysteinemia, an established risk factor for vascular disease (Shuper et al., 2002). These MTX-induced biochemical alterations are suggested to cause demyelination and endothelial cell injury resulting in leukoencephalopathy (Shuper et al., 2002).

Besides the blood-brain barrier, the blood-cerebrospinal-fluid (BCSF) barrier protects the brain from potential harmful xenobiotics, including drugs like MTX. The BCSF barrier is composed of tight-junctioned choroid plexus (CP) epithelial cells with an apical side facing the cerebrospinal-fluid (CSF) and a basolateral side facing the CP fenestrated capillaries (Spector and Johanson, 2010). The choroid plexus generally limits drug disposition of the brain parenchyma through prevention of entry of systemically administered compounds into the CSF or excretion of intrathecal applied drugs from the CSF into blood. The latter is achieved by several plasma membrane proteins expressed at the luminal side of the CP that mediate uptake of drugs from the CSF into CP cells and carrier proteins located at the basolateral membrane mediating drug efflux from the CP into blood (Spector and Johanson, 2010).

The chemotherapeutic drug MTX is a known substrate of the Reduced folate carrier (Rfc1, Slc19a1) (Matherly and Goldman, 2003) and members of the organic anion transporter (Oat)

Molecular Pharmacology Fast Forward. Published on July 7, 2011 as DOI: 10.1124/mol.111.072421
This article has not been copyedited and formatted. The final version may differ from this version.

(Anzai et al., 2006) as well as of ABC export carrier, including multidrug resistance-associated protein (Mrp) and breast cancer resistance protein (Bcrp) (Nies, 2007). Up to now, expression and subcellular localization has only been shown for rodent Rfc1 and Oat3 (Slc22a8) at the apical CP membrane as well as for Mrp1 (Abcc1) and Mrp4 (Abcc4) at the basolateral membrane of human and rodent CP (Nies 2007; Hinken et al., 2011). Oat1 (Slc22a6) was also found in rat and human CP epithelial cells, but the exact membrane localization is not clear (Nies 2007). Presence of Bcrp in the blood-CSF barrier is currently unknown (Nies 2007). It was shown previously, that uptake of MTX in CP epithelial cells is concentrative and sodium-dependent (Breen et al., 2004). However, the involvement of particular influx or efflux carrier proteins in MTX transport across the blood-CSF barrier remains unclear (Spector and Johanson, 2010).

Several studies indicate that sodium-dependent Rfc1 provides the major route for cellular uptake of MTX at neutral pH (Zhao et al., 2008, Biswal et al., 2009). We have demonstrated recently, that hepatocellular Rfc1-mediated MTX influx is significantly reduced after treatment with clinical relevant concentrations of the AEDs PB or CBZ due to posttranscriptional downregulation of the carrier protein (Halwachs et al., 2007). In childhood ALL, seizures represent a frequent clinical manifestation of MTX neurotoxicity particularly related to intrathecal MTX (Maytal et al., 1995). Besides, seizures due to metabolic disorders, cerebral infarction or CNS infection has been observed (Maytal et al., 1995). As in these patients co-medication with antiepileptic drugs (AEDs) is regularly required (Tibussek et al., 2006), we examined the contribution of Rfc1 to MTX transport at the blood-CSF barrier and investigated the effect of AEDs on Rfc1 uptake activity on the functional, transcriptional and posttranscriptional level using the rat CP-like in vitro model Z310 (Zheng and Zhao, 2002; Shi et al., 2008).

In this study, we showed expression of important MTX transporters in choroidal epithelial Z310 cells analogue to rat CP tissue. Moreover, we first illustrate subcellular localization of

Molecular Pharmacology Fast Forward. Published on July 7, 2011 as DOI: 10.1124/mol.111.072421
This article has not been copyedited and formatted. The final version may differ from this version.

Rfc1 and Bcrp at the apical CP membrane. Furthermore, our data suggested that vectorial transport of MTX across the CP is mainly achieved by Rfc1-mediated MTX uptake followed by drug efflux that very likely particularly involved Mrp1. Antiepileptic treatment with clinical relevant concentrations of the constitutive androstane receptor (CAR) agonists PB or CBZ but not non-CAR agonist gabapentin resulted in a significant reduction of Rfc1-mediated MTX uptake due to an inhibition of Rfc1 mRNA translation.

Molecular Pharmacology Fast Forward. Published on July 7, 2011 as DOI: 10.1124/mol.111.072421
This article has not been copyedited and formatted. The final version may differ from this version.

Material and Methods

Materials. All chemicals including media and supplements were obtained from Sigma-Aldrich (Deisenhofen, Germany) unless stated otherwise.

Cell culture. The immortalized Z310 rat choroidal epithelial cell line was kindly provided by Dr. Wei Zheng (Purdue University, West Lafayette, IN, USA) and has been described previously (Zheng and Zhao, 2002). Cells were maintained in Dulbecco´s modified Eagle´s medium (DMEM; PAA, Coelbe, Germany) containing 10% (v/v) fetal calf serum (Gibco, Karlsruhe, Germany), 100 U/ml penicillin, 100 µg/ml of streptomycin (PAA) and 40 µg/ml gentamycin (PAA). Polarized cell monolayers were obtained by culture on Polyester Transwell®-Clear inserts (1.0 cm^2 growth area, 0.4 µm pore size, Corning, Wiesbaden, Germany) coated with 0.01% rat tail collagen overnight. Z310 cells (2 x 10^5) were suspended in 1 ml complete growth medium supplemented with 1 µM dexamethasone (Shi and Zheng, 2005) and added to the inner chamber, which was inserted into the outer chamber containing 1.3 ml culture medium. Growth medium was exchanged daily. Formation of cell monolayer was followed by measurement of transepithelial electrical resistance (TEER) by using a low-impedance volt-ohm meter equipped with a Chopstick electrode (Millipore, Schwalbach, Germany).

Choroid plexus tissue. Samples of the lateral and fourth ventricle CP were from male Sprague-Dawley rats (200−250 g). Rats were euthanized by asphyxiation with CO_2, brains were removed, and CPs then excised. These procedures were conducted in the central animal facility of the Medical Faculty of the Universität Leipzig according to institutional guidelines for ethical care and use of animals for experimental and other scientific purposes.

Molecular Pharmacology Fast Forward. Published on July 7, 2011 as DOI: 10.1124/mol.111.072421
This article has not been copyedited and formatted. The final version may differ from this version.

RT-PCR. Total RNA was prepared from CP and 5×10^6 Z310 cells grown to confluence using the SV Total RNA Isolation System (Promega, Madison, WI, USA) according to the manufacturer's instructions. Total RNA (1 µg) was used to synthesize cDNA under standard conditions employing the First Strand cDNA Synthesis Kit for RT-PCR (Fermentas, St. Leon-Rot, Germany) with 20 U of reverse transcriptase (M-MuLV RT) and 25 µg oligo $(dT)_{18}$ primer. PCR amplification was carried out using 1/25 of cDNA, 0.2 mM mixed dNTPs, and 1.5 U DreamTaq DNA polymerase (Fermentas). Specific primers for rOat3, rOatp1a5, rPCFT, rMrp1, rMdr1, and rBcrp were designed using PrimerSelect software (DNAStar Inc., Madison, WI, USA). All gene specific primer pairs and annealing temperatures are listed in the Supplemental Table 1S. PCR was performed over 32 cycles with an initial denaturation step of 30 sec at 95°C followed by annealing and extension at 72°C for 40 sec. A final extension was carried out at 72°C for 5 min. The PCR products were analysed by agarosegel electrophoresis with regard to size of the expected fragment. G3PDH was used as positive control and amplification of genomic DNA was excluded by omitting reverse transcriptase.

Quantitative RT-PCR of Rfc1 gene expression. Total RNA was prepared from 5×10^6 Z310 cells grown to confluence using the RNeasy Mini system (Qiagen, Hilden, Germany) according to the manufacturer's instructions and cDNA was synthesized from total RNA (1 µg) as delineated above. Quantitative PCR of 1 µl cDNA was carried out using the PCR-Master-Mix S (peqlab, Erlangen, Germany) as well as Rfc1 specific sense and antisense primers and TaqMan probe as described previously (Halwachs et al., 2007). Rfc1 mRNA expression relative to the normalized (β-actin) control level was calculated by the $2^{-\Delta\Delta CT}$ method, taking the Rfc1 PCR efficacy into account.

SDS-PAGE and Western Blot analysis. Z310 cells were harvested in lysis buffer (50 mM Tris-HCl, pH 7.4, 150 mM NaCl, 1% Triton X-100, 0.5% sodium desoxycholate, 2 mM

Molecular Pharmacology Fast Forward. Published on July 7, 2011 as DOI: 10.1124/mol.111.072421
This article has not been copyedited and formatted. The final version may differ from this version.

sodium vanadate, 1 X protease inhibitor cocktail) and incubated for 60 min on ice. Nuclei and cell debris were pelleted at 1000 x g for 5 min at 4 °C. Protein concentrations were measured using the BCA protein assay (Pierce, Rockford, IL, USA). Whole cell lysates were mixed in sample buffer (final: 2% SDS, 10% (v/v) glycerol, 50 mM Tris-HCl, 0.1% bromphenol blue, pH 6.8) and apart from Rfc1 supplemented with ß-mercaptoethanol (100 mM). For detection of Oat1, proteins were denaturated at 37°C for 30 min. According to protein size equal protein amounts were separated on SDS/7.5% polyacrylamide gel for Oat3, Mrp1 and Bcrp or 10% SDS gels for Oat1, Rfc1 and ß-actin. Subsequently, proteins were blotted onto nitrocellulose membrane. Unspecific binding was blocked with 5% milk powder in TBS-Tween (TBST: 20 mM Tris-HCl, pH 7.5, 150 mM NaCl, 0.5% (v/v) Tween 20) for 1 h at room temperature. Membranes were probed overnight at 4 °C in 3% milk powder in TBST with the following primary antibodies: polyclonal anti-rat OAT1 (Ab-1; 2.5 µg/ml; kindly provided by BC Burckhardt, Georg-August University of Göttingen, Germany), polyclonal anti-OAT3 (H-44; 1:200; Santa Cruz, Heidelberg, Germany), polyclonal anti-SLC19A1 (1:100; Abcam Inc, Cambridge, MA, USA), anti-MRP1 MAb (MRPr1; 1:20; generous gift from G Fricker, Ruprecht-Karls-University, Heildelberg, Germany) anti-ABCG2 MAb (BXP-21; 1:100; Santa Cruz) or anti-ß-actin MAb (1:10,000; clone AC-15). As secondary antibodies, AP-conjugated goat anti-mouse IgG (1:7,000; Promega, Madison, WI, USA) for Bcrp and ß-actin, AP-conjugated goat anti-rat IgG (1:5000; Santa Cruz) for Mrp1 or AP-conjugated goat anti-rabbit IgG (1:2000; Dako Cytomation, Hamburg, Germany) for Oat1, Oat3 and Rfc1 were used. Transporter-antibody complexes were visualized using Western Blue® stabilized substrate for alkaline phosphatase (Promega). Densitometric quantification of Rfc1 protein was performed with 1D Image Analysis Software (GeneTools, Syngene, Cambridge, UK). The amount of Rfc1 in the presence of PB in consideration of the background level was expressed as the x-fold change compared to untreated Z310 cells.

Molecular Pharmacology Fast Forward. Published on July 7, 2011 as DOI: 10.1124/mol.111.072421
This article has not been copyedited and formatted. The final version may differ from this version.

Immunocytochemical analysis. Z310 cells were cultured on Transwell®-inserts as delineated above. Cells were fixed in acetone (-20 °C) for 10 min and permeabilised with 0.001% (v/v) Triton X-100. Unspecific binding was blocked with 5% (v/v) BSA in PBS. Samples were incubated overnight at 4 °C with anti-SLC19A1 (1:30), BXP-21 (1:100), MRPr1 (1:20) or TJP-1 (1:200) for ZO-1 following visualization by goat anti-rabbit Alexa 488 IgG (1:400; Molecular Probes, Eugene, OR, USA) for Rfc1 and ZO-1, goat anti-mouse Alexa 594 IgG (1:400; Molecular Probes) for Bcrp or DyLight™649-conjugated donkey anti-rat IgG (1:500; Jackson ImmunoResearch Laboratories Inc., West Grove, PA, USA) for Mrp1 over 1.5 h at room temperature. Nuclear staining was achieved by addition of 4'-6-Diamidino-2-phenylindole (DAPI; 0.5 µg/ml). Finally, the specimens were washed and mounted on slides with Fluoromount. Control incubations were generally performed by omission of primary antibodies. Confocal images of Z310 cells were taken by sequential scanning of optical sections (XY) of about 0.13 µm thickness.

Confocal Laser Scanning Microscopy. Cell samples were analysed using the inverted confocal laser scanning microscope Leica TCS SP5 equipped with a HCX PL APO 63x 1.4 oil immersion objective (Leica Microsystems, Wetzlar, Germany). All images were acquired in the sequential scan mode using an argon laser at 488 nm wavelength (to visualize Alexa 488), a helium-neon laser at 594 nm or at 633 nm (to visualize Alexa 594 or DyLight™649) or an UV-diode laser at 405 nm (to visualize DAPI). Image stacks were processed and analysed with the LAS AF1.7.0 software (Leica Microsystems, Wetzlar, Germany) and Adobe Photoshop 6.0.

Pre-treatment of Z310 cells. In order to investigate the effect of AEDs on Rfc1 uptake activity, cells were treated with PB (43 or 430 µM), CBZ (12.7 or 127 µM) or gabapentin (11.7 or 117 µM) in supplemented DMEM for 48 h. Selected concentrations of the respective

Molecular Pharmacology Fast Forward. Published on July 7, 2011 as DOI: 10.1124/mol.111.072421
This article has not been copyedited and formatted. The final version may differ from this version.

drugs comply with the therapeutic plasma level in humans (Patsalos, 1999; Meyer, 2004) and the decuple of this concentration. Medium was changed every 24 h to maintain stable effective concentrations.

Uptake assays. Measurements of [^{3}H] methotrexate ([^{3}H] MTX; specific activity: 6.18 x 10^8 kBq/mmol; Moravek Biochemicals, Brea, CA, USA) uptake in Z310 cells were carried out by a modified method described previously (Halwachs et al., 2007). Intracellular MTX accumulation was generally examined after cells were harvested and allowed to recover in fresh culture medium for 20 min. In all cases, cell viability was ≥ 92% as assessed by trypan blue exclusion. Z310 cells were washed 3 times in artificial cerebrospinal-fluid (aCSF: 103 mM NaCl, 4.7 mM KCl, 2.5 mM $CaCl_2$, 1.2 mM KH_2PO4, 1.2 mM $MgSO_4$, 25 mM $NaHCO_3$, 10 mM glucose, and 1 mM sodium pyruvate, pH 7.4) (Breen et al., 2004). For sodium-free aCSF, NaCl was replaced by choline chloride and $NaHCO_3$ by choline bicarbonate as previously delineated (Breen et al., 2004). Subsequently, [^{3}H] MTX (5 µM, 2 × 10^5 dpm/ml) was added to 1.2 ml cell suspension. The aliquots (100 µl) were removed at 0.25; 0.75; 1.25; 3; 5; 10; 20 min for determination of ABC transporter-mediated efflux activity. For investigation of MTX influx, cells were loaded with MTX as performed for the efflux studies but samples were collected only over a short time period at 0.25; 0.75; 1.20; 1.5; 2 ; 2.5 min. To obtain Michaelis-Menten uptake parameters, non-labeled MTX at a concentration of up to 10 µM was added to the cell suspension and intracellular drug accumulation was measured over 3 min. Then, cells were separated by centrifugation through a silicon oil cushion. The pelleted cells were dissolved in 4 M KOH overnight and the cell-associated radioactivity was measured by liquid scintillation counting (LS 6500, Beckman, Fullerton, CA). Protein concentration of the cell suspension was measured using the bicinchoninic (BCA) protein assay.

Molecular Pharmacology Fast Forward. Published on July 7, 2011 as DOI: 10.1124/mol.111.072421
This article has not been copyedited and formatted. The final version may differ from this version.

Kinetic and statistical analyses. Statistical analysis of all data was carried out using Microsoft Excel software (Office 2000). K_m and V_{max} values were obtained with Prism 4.0 (GraphPad Software Inc., San Diego, CA) by fitting to the Michaelis-Menten equation using the least square method and confirmed by Lineweaver-Burk plot. Curve fittings were performed by means of SigmaPlot 10 (Systat Software Inc.). Student's *t*-test was used to determine the significance of differences between respective test series. Statistical significance was assumed at p values of < 0.05.

Molecular Pharmacology Fast Forward. Published on July 7, 2011 as DOI: 10.1124/mol.111.072421
This article has not been copyedited and formatted. The final version may differ from this version.

Results

Expression of organic anion transporters in Z310 cells. To obtain an overview about the constitutive expression of various organic anion transporters in the Z310 cell line, we performed RT-PCR analyses and compared the expression profile to that from rat CP that served as a positive control. As illustrated in Fig. 1A, transcripts for Oat1, Oat3, Rfc1, FOLR, PCFT, Mrp1, Mrp3, Mrp4, Mrp5, Mdr1, and Bcrp were detected in Z310 cells. This expression profile was almost identical to that found for rat CP, with exception of Oatp1a4 and Oatp1a5. RNA of the latter was undetectable in the Z310 cell line. Conversely, mRNA levels of Mdr1 were at the limit of detection in CP tissue whereas a strong signal for Mdr1 was obtained in Z310 cells. When comparing the apparent level of gene expression for MTX transporter between the RNA sources, Oat1, Oat3 and FOLR expression can be ranked higher in rat CP tissue than in Z310 cells. On the contrary, higher mRNA levels were demonstrated for Rfc1 and the detected Mrp efflux transporter in the Z310 cell line compared to rat CP.

The influx carriers Rfc1 and Oat3 as well as efflux transporters Mrp1 and Mrp4 have been recently suggested to be involved in MTX transport across the blood-CSF barrier in human and rodent (Nies, 2007; Spector and Johanson, 2010). As MTX has been also identified as a substrate for Oat1 and Bcrp, we investigated protein expression of Oat1, Oat3, Rfc1, Mrp1, and Bcrp in Z310 cells. Detection of Pgp was neglected as MTX has not been identified as a substrate of this efflux carrier (Jansen et al., 2003). As shown in Fig. 1B, Oat3 protein was found at molecular weights of ~ 130 kDa as described previously (Srimaroeng et al., 2008). Oat1 protein could not be detected in Z310 cells. As Oat1 was found only to a minor degree at the RNA level the Oat1 protein is probably below detectability as similarly observed for rat CP tissue (Nies, 2007). Specific anti-Rfc antibody labeled a band for Rfc1 of ~ 56 kDa (Fig. 1B) corresponding to the non-glycosylated form of the carrier protein as found in rat liver (Honscha et al., 2000). This band was completely blocked by the respective peptide (Hinken

Molecular Pharmacology Fast Forward. Published on July 7, 2011 as DOI: 10.1124/mol.111.072421
This article has not been copyedited and formatted. The final version may differ from this version.

et al., 2011) corroborating specificity of antibody labeling (not shown). In regard to the expression of main MTX efflux carriers at the protein level, specific bands at 72 kDa for Bcrp and 190 kDa for Mrp1 were detected in Z310 cells (Fig. 1B).

Subcellular localisation of Rfc1, Bcrp and Mrp1 protein in polarized Z310 monolayers. Z310 cells were grown on Transwell filter inserts as described above. After four days in culture, polarized cell monolayers were obtained with TEER values (91.00 ± 5.94 Ω cm^2) in the same range as shown previously (Shi et al., 2008). Cell layers were fixed and examined for subcellular distribution of Rfc1, Bcrp or Mrp1 protein via XY sectioning by confocal microscopy. Formation of monolayer barriers in the Z310 model was additionally assessed by detection of the tight junction protein ZO-1 (Fig. 2C). As shown in Fig. 2A and 2B, Rfc1 is predominantly localized at the apical plasma membrane of Z310 cells. Similarly, specific staining for Bcrp was mainly observed at the apical membrane in choroidal epithelial cells (Fig. 2A and 2B). Besides, Bcrp was detected by confocal microscopy in XZ views partially between cell nuclei suggesting lateral localization of Bcrp protein (Fig. 2A). In contrast, Mrp1 was predominantly found at the basolateral membrane of Z310 cells (Fig. 2C). Tight junction protein ZO-1 was detected at the lateral plasma membrane (Fig. 2C).

MTX transport in Z310 cells. In order to identify carriers involved in transepithelial transport of MTX in rat CP, we measured the impact of various substances known to interact specifically with organic anion transporters on intracellular MTX accumulation in Z310 cells. In untreated control cells, MTX uptake rapidly reached a maximum over up to 3 min (Fig. 3). This initial uptake interval was generally followed by a rapid decline in intracellular MTX accumulation (Fig. 3, 4), with low steady state levels attained after 10 min corresponding to

Molecular Pharmacology Fast Forward. Published on July 7, 2011 as DOI: 10.1124/mol.111.072421
This article has not been copyedited and formatted. The final version may differ from this version.

by on average 21% of the maximum cellular MTX content at the end of the uptake phase (3 min) (Fig. 4).

Several studies indicate that Rfc1 represents the major pathway for the uptake of MTX at neutral pH (Zhao et al., 2008, Biswal et al., 2009). Rfc1-mediated but not PCFT- or FORL-dependent MTX influx is strictly sodium-dependent at pH 7.4 (Kneuer and Honscha, 2004; Halwachs et al., 2005). To determine the involvement of Rfc1 in MTX uptake from the CSF into CP, we therefore investigated MTX accumulation in Z310 cells over 5 min in the presence or absence of extracellular sodium. As shown in Fig. 3A, incubation of cells in sodium-depleted aCSF caused a significant reduction in MTX uptake by up to 81% within the initial uptake interval. Rfc1-mediated MTX influx was further confirmed using 5-MTHF. Incubation with both concentrations of the competitive Rfc1 inhibitor (Matherly and Goldman, 2003) almost completely abolished intracellular MTX accumulation within the initial uptake interval (Fig. 3B). MTX uptake was saturable with a K_m of 10.1 ± 3.3 µM and a V_{max} of 95.8 ± 18.3 pmol/mg protein (Supplemental Fig. 1S). Contribution of Oat1 and Oat3 to MTX uptake into CP was assessed by incubation of Z310 cells with PAH a known substrate of Oat1 and Oat3 (Anzai et al., 2006). PAH had no effect on MTX accumulation at 0.5 mM and only inhibited MTX uptake to a minor predominantly not significant extent at a very high concentration (1 mM) (Supplemental Fig. 2S).

The leukotriene LTD_4 receptor antagonist 3-([{3-(2-[7-chloro-2-quinolinyl]ethenyl) phenyl}-{(3-dimethylamino-3-oxopropyl)-thio-methyl]thio)propanoic acid (MK571) has been previously shown to inhibit MTX transport by the Mrp family members Mrp1, Mrp3, and Mrp4, but not Mrp 5 in various cell lines (Zeng et al., 2001; Chen et al., 2002). In order to investigate the involvement of these Mrp efflux carriers in MTX transport across the blood-CSF barrier, MTX accumulation was measured over 20 min in the presence or absence of MK571. Following the initial uptake phase (3 min), addition of MK571 caused a dose-

Molecular Pharmacology Fast Forward. Published on July 7, 2011 as DOI: 10.1124/mol.111.072421
This article has not been copyedited and formatted. The final version may differ from this version.

dependent inhibition of the decline in cellular MTX levels compared to untreated control cells (Fig. 4A). Furthermore, MK571-dependent MTX accumulation rapidly attained a plateau phase after 5 min with significantly increased steady-state levels within 10 min compared to the control. Contribution of Bcrp to transepithelial transport of MTX in CP was determined by incubation of cells with the specific Bcrp inhibitor 3-((3S,6S,12aS)-6-Isobutyl-9-methoxy-1,4-dioxo-1,2,3,4,6,7,12,12a-octahydro-pyrazino[1',2':1,6] pyrido[3,4-b]indol-3-yl)-propionic acid tert-butyl ester (Ko143) (Allen et al., 2002). Addition of Ko143 caused a significant increase in steady-state MTX accumulation achieving a significant augmented plateau level after 5 min in relation to the untreated control (Fig. 4B).

Effect of AEDs on MTX uptake. To investigate the influence of the CAR-inducing AEDs PB and CBZ on Rfc1-mediated MTX uptake from the CSF into CP epithelium, Z310 cells were pre-treated with one-fold or ten-fold therapeutic plasma concentrations of PB or CBZ for 48 h. Incubation with the AED gabapentin lacking CAR-inducing activity (Tibussek et al., 2006) served as a negative control.

At neutral pH as existing at the blood-CSF barrier, human and rodent Rfc1 mediate uptake of MTX in a sodium-dependent manner (Kneuer and Honscha, 2004; Halwachs et al., 2005). Hence, the intracellular MTX accumulation was initially measured in aCSF containing 129 mM Na^+ as the overall (Na^+-dependent and Na^+-independent) MTX uptake or in sodium-free aCSF representing solely the Na^+-independent MTX accumulation rate. Subsequently, Rfc1 activity was defined indirectly as the difference of [^{3}H]-MTX uptake over 2.5 min in the presence or absence of extracellular sodium. Finally, sodium- and time-dependent Rfc1 activity was expressed in pmol per mg protein.

As illustrated in Fig. 5A, pre-treatment with therapeutic plasma concentrations (43 µM) of PB significantly reduced sodium-dependent Rfc1-mediated MTX uptake (by approximately

Molecular Pharmacology Fast Forward. Published on July 7, 2011 as DOI: 10.1124/mol.111.072421
This article has not been copyedited and formatted. The final version may differ from this version.

85%; $p < 0.001$) within the initial uptake interval (2.5 min) compared to the untreated control. Moreover, incubation of cells with 430 μM PB almost completely abolished Rfc1-dependent MTX influx. Similar results were obtained by pre-treatment with 12.7 and 127 μM CBZ (Fig. 5B). In contrast, incubation of cells with 11.7 or 117 μM gabapentin was not related to a significant alteration in Rfc1-mediated MTX uptake (Fig. 5C). The sodium-independent accumulation of the drug was generally not significantly affected (not shown).

Impact of PB on Rfc1 gene expression. To determine whether reduction of Rfc1-mediated MTX uptake by CAR-inducing AEDs is due to a decrease in Rfc1 gene expression, Rfc1 transcript levels were measured by quantitative RT-PCR. The amount of Rfc1 mRNA was normalized to the level of β-actin. As shown in Fig. 6A, pre-treatment of Z310 cells (48 h) with one-fold or ten-fold therapeutic serum levels of prototypical CAR inducer PB was not related to a significant alteration in relative Rfc1 gene expression compared with the untreated control.

Effect of PB on the Rfc1 protein level. In a further series of experiments on the regulatory mechanism of Rfc1 activity, we measured the effect of PB pre-treatment on Rfc1 protein levels in Z310 cells by Western blot. Densitometric analysis of Rfc1 specific bands showed that treatment with 43 μM PB or 430 μM PB for 48 h resulted in a concentration-dependent significant decline in the Rfc1 protein amount to 33.14% and 18.50%, respectively, of the untreated control level (Fig. 6B).

Molecular Pharmacology Fast Forward. Published on July 7, 2011 as DOI: 10.1124/mol.111.072421
This article has not been copyedited and formatted. The final version may differ from this version.

Discussion

Chemotherapy with intrathecal MTX has been linked to severe neurotoxicity in patients with ALL or lymphoma. Interestingly, clinical studies indicated that this may be due to a decrease in the CSF clearance of the drug (Bleyer et al., 1973; Ettinger, 1982, Ettinger et al., 1982). So, patients who received intrathecal MTX suffering from neurotoxicity showed by on average 13.8-fold elevated CSF drug levels compared to patients without toxicity (Bleyer et al., 1973). MTX is known to be actively secreted from CSF into blood but the carrier proteins involved remain undefined (Spector and Johanson, 2010).

In this study we show that the mRNA expression pattern of organic anion transporters in rat choroidal epithelial Z310 cells was almost identical to that of rat choroid plexus tissue. Endogenous transporter expression included the known MTX import carrier Oat1, Oat3, Rfc1, and PCFT (Slc46a1) as well as the folate-binding protein FORL (Matherly and Goldman, 2003; Nies 2007; Inoue et al., 2008). Compared to rat CP, lower expression of Oat1 and Oat3 in Z310 cells must be discussed in the context of gender and hormone dependency as murine Oat1 expression was higher in male than in female kidney and rat Oat3 was only detected in male liver (Anzai et al., 2006). As the culture of Z310 cells generated from both sexes of Sprague-Dawley rats was carried out without supplementation of male sex hormones it is likely that expression of both transporters could be inducible by testosterone. However, high concentrations of the high affinity Oat1 and Oat3 substrate PAH (Anzai et al., 2006) had only a minor mainly non-significant effect on MTX uptake. In line with previous data on the effect of PAH on MTX uptake in rat CP tissue (Breen et al., 2004), our results therefore indicate that Oat transporters do not play a significant role in MTX removal from the CSF.

As MTX uptake was almost completely abolished in the presence of 5-MTHF and displayed to be strictly sodium-dependent our results rather suggest that Rfc1 provides the main route for MTX uptake in Z310 cells. This is in line with previous data showing that MTX uptake in rat CP tissue was specific, concentrative and sodium-dependent (Breen et al.,

Molecular Pharmacology Fast Forward. Published on July 7, 2011 as DOI: 10.1124/mol.111.072421
This article has not been copyedited and formatted. The final version may differ from this version.

2004). Our data is further corroborated by the apical membrane localization of Rfc1 in Z310 cells supporting recent findings of subcellular distribution of Rfc1 in rat CP tissue (Hinken et al., 2011). Several publications clearly demonstrated that at neutral pH PCFT-mediated MTX transport in various cell lines is negligible (Inoue et al., 2008; Zhao et al., 2008). This data is confirmed by results derived in liver-like Huh7 cells transfected with Rfc siRNA showing that MTX transport at neutral pH is mediated largely by Rfc1 (Biswal et al., 2009). The FOLR is localized to the basolateral CP membrane and in contrast to 5-MTHF exhibits a relatively low affinity for MTX (Spector and Johanson, 2010). Thus, significant involvement of PCFT or FOLR in removal of MTX from CSF is not likely.

In line with recent data on endogenous expression of Mrp efflux transporters in isolated rat CP (Choudhuri et al., 2003) various Mrp family members were identified with predominant expression of Mrp1 in CP tissue and in Z310 cells. Our results obtained with specific Mrp inhibitor MK571 (Zeng et al., 2001; Chen et al., 2002) suggested the involvement of Mrp1, Mrp3 and Mrp4 in elimination of MTX from Z310 cells. This suggestion is corroborated by expression of Mrp1 protein at the basolateral membrane of Z310 cells. Similarly, Mrp4 also expressed in Z310 cells (Kläs et al., 2010) has been localized to the basolateral CP membrane (Nies, 2007). Moreover, functional activity of both transporters has been recently shown in Z310 cells using specific subfamily member substrates (Kläs et al., 2010). No information is as yet available on the functional expression and subcellular distribution of Mrp3 protein. Though, as Mrp3 mRNA was detected in rat CP tissue and Z310 cells, contribution of Mrp3 to elimination of MTX can not be excluded. However, in regard to the predominant expression and the strong effect of the potent Mrp1-inhibitor MK571 (Leier et al., 1996) on MTX accumulation, we suggest that Mrp1 is the prevailing Mrp family member responsible for MTX efflux in Z310 cells.

To our knowledge this is the first report illustrating subcellular localization of Bcrp at the apical membrane of choroidal epithelial cells. Bcrp-mediated efflux of MTX in these cells

Molecular Pharmacology Fast Forward. Published on July 7, 2011 as DOI: 10.1124/mol.111.072421
This article has not been copyedited and formatted. The final version may differ from this version.

was confirmed using the specific Bcrp inhibitor Ko143 (Allen et al., 2002). As Bcrp-mediated efflux of intracellular synthesized oligoglutamate MTX derivatives has been previously shown in several tumour cell lines (Assaraf, 2006), our results suggested that apically expressed Bcrp may facilitate MTX accumulation in CSF. Though, our data argue for Mrp1 as the primary active MTX efflux transporter in choroid plexus as intracellular drug accumulation by Mrp1- inhibitor MK571 was twice the level as observed with Bcrp inhibitor Ko143. However, specific inhibitors of Bcrp activity may be useful tools to reduce neurotoxicity of intrathecally administered MTX by facilitating Mrp1-mediated drug removal from CSF into blood.

In patients with ALL or lymphoma, intrathecal MTX-induced neurotoxicity usually manifest as seizure requiring treatment with AEDs. Interestingly, we have recently shown that clinically relevant concentrations of PB or CBZ cause significant downregulation of hepatocellular Rfc1 uptake activity through activation of the CAR signalling pathway (Halwachs et al., 2007; Halwachs et al., 2009). The nuclear receptor CAR is known to mediate regulation of carrier associated drug transport by PB or CBZ through modulation of target gene expression, including MTX efflux transporter Mrp2 (Xu et al., 2005). In fact, our results displayed that Rfc1-meditated MTX uptake in CP epithelial cells is significantly decreased by therapeutic serum concentrations of PB or CBZ. However, our data indicate that this reduction was not due to altered carrier gene expression. Similarly, long-term treatment of human ovarian carcinoma cells with CBZ significantly reduced Rfc-mediated MTX uptake, but was not associated with decreased Rfc transcript levels (Toffoli et al., 2000). In addition to regulation of gene expression, PB-induced regulation of protein levels is known to affect membrane transporters such as Mrp2 (Johnson et al., 2002). Indeed, pre-treatment of Z310 cells with PB resulted in a significant reduction in relative Rfc1 protein levels. Therefore, our results suggest that regulation of Rfc1 uptake activity by CAR-inducing AEDs does not occur via CAR-dependent transcriptional regulation but by inhibition of carrier translation on the

Molecular Pharmacology Fast Forward. Published on July 7, 2011 as DOI: 10.1124/mol.111.072421
This article has not been copyedited and formatted. The final version may differ from this version.

posttranscriptional level. This lack of response on the transcriptional level may be explained by absence of the CAR response element "phenobarbital response enhancer module (PBREM)" involved in PB-dependent induction of CYP450 enzymes (Xu et al., 2005) from the rfc1 gene 5`-flanking region (Honscha et al., 2000).

Altogether, this study provides data on the functional expression of MTX import and export carriers in choroidal epithelial cells. Our results further indicate that removal of intrathecally applied MTX across the blood-CSF barrier may be achieved through a two-step mechanism of transepithelial transport that includes Rfc1-mediated uptake from the CSF at the apical CP membrane followed by MTX extrusion into blood particularly via Mrp1 at the basolateral membrane. In this study, this two-step transport mechanism was illustrated by a bell-shaped transport curve reflecting a short uptake phase with intracellular MTX accumulation succeeded by avid drug efflux resulting in a rapid decline in cellular MTX levels. A similar curve shape was recently reported for MTX accumulation in rat CP tissue (Breen et al., 2004). As human RFC1 and rat Rfc1 has been shown to be orthologs (Kneuer and Honscha, 2004) a broader relevance of our results to other systems including human cells can be assumed. In consideration of the known dose-dependency of MTX toxicity (Shuper et al., 2002), one therefore may suggest that PB or CBZ-induced downregulation of Rfc1 may induce intrathecal MTX neurotoxicity in patients with cancer-related seizures or potentiate drug toxicity in patients with MTX-induced seizures by a decrease in CSF clearance of the drug. As we show that gabapentin did not lead to significant changes in Rfc1-mediated MTX uptake, new non CAR-inducing AEDs like gabapentin (Tibussek et al., 2006) should therefore be preferred for seizure control. Finally, consideration of drug interactions by regulation of carrier-mediated transport may help to improve antiepileptic treatment in children with ALL receiving intrathecal MTX chemotherapy.

Molecular Pharmacology Fast Forward. Published on July 7, 2011 as DOI: 10.1124/mol.111.072421
This article has not been copyedited and formatted. The final version may differ from this version.

Acknowledgements

We thank Wei Zheng (Purdue University, West Lafayette, IN, USA) for donating the Z310 cell line. We also thank G. Fricker (Ruprecht-Karls-University, Heildelberg, Germany) for generously providing the anti-Mrp1 antibody and B.C. Burckhardt (Georg-August University of Goettingen, Goettingen, Germany) for kindly providing the anti-Oat1 antibody.

Molecular Pharmacology Fast Forward. Published on July 7, 2011 as DOI: 10.1124/mol.111.072421
This article has not been copyedited and formatted. The final version may differ from this version.

Authorship Contributions

Participated in research design: S. Halwachs, W. Honscha

Conducted experiments: S. Halwachs, C. Lakoma

Contributed new reagents or analytical tools: I. Schäfer, P. Seibel

Performed data analysis: S. Halwachs

Wrote or contributed to the writing of the manuscript: S. Halwachs, W. Honscha

Molecular Pharmacology Fast Forward. Published on July 7, 2011 as DOI: 10.1124/mol.111.072421
This article has not been copyedited and formatted. The final version may differ from this version.

References

Allen JD, van Loevezijn A, Lakhai JM, van der Valk M, van Tellingen O, Reid G, Schellens JH, Koomen GJ, and Schinkel AH (2002) Potent and specific inhibition of the breast cancer resistance protein multidrug transporter in vitro and in mouse intestine by a novel analogue of fumitremorgin C. *Mol Cancer Ther* **1:** 417-425.

Anzai N, Kanai Y, and Endou H (2006) Organic anion transporter family: current knowledge. *J Pharmacol Sci* **100:** 411-426.

Assaraf YG (2006) The role of multidrug resistance efflux transporters in antifolate resistance and folate homeostasis. *Drug Resist Updat* **9:** 227-246.

Biswal BK, and Verma RS (2009) Differential usage of the transport systems for folic acid and methotrexate in normal human T-lymphocytes and leukemic cells. *J Biochem* **146:** 693-703.

Bleyer WA, Drake JC, and Chabner BA (1973) Neurotoxicity and elevated cerebrospinal-fluid methotrexate concentration in meningeal leukemia. *N Engl J Med* **289:** 770-773.

Breen CM, Sykes DB, Baehr C, Fricker G, and Miller DS (2004) Fluorescein-methotrexate transport in rat choroid plexus analyzed using confocal microscopy. Am J Physiol Renal Physiol **287**: F562-F569**.**

Chen ZS, Lee K, Walther S, Raftogianis RB, Kuwano M, Zeng H, and Kruh GD (2002) Analysis of methotrexate and folate transport by multidrug resistance protein 4 (ABCC4): MRP4 is a component of the methotrexate efflux system. *Cancer Res* **62**: 3144-3150.

Choudhuri S, Cherrington NJ, Li N, and Klaassen CD (2003) Constitutive expression of various xenobiotic and endobiotic transporter mRNAs in the choroid plexus of rats. *Drug Metab Dispos* **31**: 1337-1345.

Ettinger LJ (1982) Pharmacokinetics and biochemical effects of a fatal intrathecal methotrexate overdose. *Cancer* **50**: 444-450.

Ettinger LJ, Chervinsky DS, Freeman AI, Creaven PJ (1982) Pharmacokinetics of methotrexate following intravenous and intraventricular administration in acute lymphocytic leukemia and non-Hodgkin's lymphoma. Cancer. *Cancer* **50**: 1676-1682.

Halwachs S, Kneuer C, Honscha W (2005) Endogenous expression of liver-specific drug transporters for organic anions in the rat hepatocytoma fusion cell line HPCT-1E3. *Eur J Cell Biol* **84**: 677-686.

Halwachs S, Kneuer C, and Honscha W (2007) Downregulation of the reduced folate carrier transport activity by phenobarbital-type cytochrome P450 inducers and protein kinase C activators. *Biochem Biophys Acta* **1768:** 1671-1679.

Halwachs S, Schäfer I, Seibel P, and Honscha W (2009) Antiepileptic drugs reduce efficacy of methotrexate chemotherapy by downregulation of Reduced folate carrier transport activity. *Leukemia* **23:** 1087-1097.

Hinken M, Halwachs S, Kneuer C, and Honscha W (2011) Subcellular localization and distribution of the reduced folate carrier in normal rat tissues. *Eur J Histochem* **55**: e3.

Honscha W, Dötsch KU, Thomsen N, and Petzinger E (2000) Cloning and functional characterization of the bile acid-sensitive methotrexate carrier from rat liver cells. *Hepatology* **31:** 1296-1304.

Inoue K, Nakai Y, Ueda S, Kamigaso S, Ohta KY, Hatakeyama M, Hayashi Y, Otagiri M, and Yuasa H (2008) Functional characterization of PCFT/HCP1 as the molecular entity of the carrier-mediated intestinal folate transport system in the rat model. *Am J Physiol Gastrointest Liver Physiol* **294:** G660-G668.

Jansen G, Scheper RJ, Dijkmans BA (2003) Multidrug resistance proteins in rheumatoid arthritis, role in disease-modifying antirheumatic drug efficacy and inflammatory processes: an overview. *Scand J Rheumatol* **32**: 325-336.

Johnson DR, Habeebu SS, and Klaassen CD (2002) Increase in bile flow and biliary excretion of glutathione-derived sulfhydryls in rats by drug-metabolizing enzyme inducers is mediated by multidrug resistance protein 2. *Toxicol Sc* **66:** 16-26.

Kläs J, Wolburg H, Terasaki T, Fricker G, and Reichel V (2010) Characterization of immortalized choroid plexus epithelial cell lines for studies of transport processes across the blood-cerebrospinal fluid barrier. *Cerebrospinal Fluid Res* **7:** 11.

Kneuer C, and Honscha W (2004) The $H^{(+)}$-dependent reduced folate carrier 1 of humans and the sodium-dependent methotrexate carrier-1 of the rat are orthologs. *FEBS Lett* **566:** 83-86.

Kwong YL, Yeung DY, and Chan JC (2009) Intrathecal chemotherapy for hematologic malignancies: drugs and toxicities. *Ann Hematol* **88:** 193-201.

Leier I, Jedlitschky G, Buchholz U, Center M, Cole SP, Deeley RG, and Keppler D (1996) ATP-dependent glutathione disulphide transport mediated by the MRP gene-encoded conjugate export pump. *Biochem J* **314**: 433-437.

Matherly LH, and Goldman ID (2003) Membrane transport of folates. *Vitam Horm* **66:** 403-456.

Maytal J, Grossman R, Yusuf FH, Shende AC, Karayalycin G, Lanzkowsky P, Schaul N, and Eviatar L (1995) Prognosis and treatment of seizures in children with acute lymphoblastic leukemia. *Epilepsia* **36:** 831-836.

Meyer FP (1994) Indicative therapeutic and toxic drug concentrations in plasma: a tabulation. *Int J Clin Pharmcol Ther* **32**: 71-81.

Nies AT (2007) The role of membrane transporters in drug delivery to brain tumors. *Cancer Lett* **254:** 11-29.

Patsalos PN (1999) New antiepileptic drugs. *Ann Clin Biochem* **36**: 10-19.

Shi LZ, Li GJ, Wang S, and Zheng W (2008) Use of Z310 cells as an in vitro blood-cerebrospinal fluid barrier model: tight junction proteins and transport properties. *Toxicol In Vitro* **22**: 190-199.

Shi LZ, and Zheng W (2005) Establishment of an in vitro brain barrier epithelial transport system for pharmacological and toxicological study. *Brain Res* **1057**: 37-48.

Shuper A, Stark B, Kornreich L, Cohen IJ, Avrahami G, and Yaniv I (2002) Methotrexate-related neurotoxicity in the treatment of childhood acute lymphoblastic leukemia. *Isr Med Assoc J* **4:** 1050-1053.

Spector R, and Johanson CE (2010) Vectorial ligand transport through mammalian choroid plexus. *Pharm Res* **27**: 2054-2062.

Srimaroeng C, Perry JL, and Pritchard JB (2008) Physiology, structure, and regulation of the cloned organic anion transporters. *Xenobiotica* **38**: 889-935.

Tibussek D, Distelmaier F, Schönberger S, Göbel U, and Mayatepek E (2006) Antiepileptic treatment in paediatric oncology--an interdisciplinary challenge. *Klin Padiatr* **218:** 340-349.

Toffoli G, Corona G, Tolusso B, Sartor F, Sorio R, Mini E, and Boiocchi M (2000) Resistance to methotrexate in SKOV-3 cell lines after chronic exposure to carbamazepine is associated with a decreased expression of folate receptor. *Int J Cancer* **85:** 683-690.

Xu C, Li CY, and Kong AN (2005) Induction of phase I, II and III drug metabolism/transport by xenobiotics. *Arch Pharm Res* **28:** 249-268.

Zhao R, Qiu A, Tsai E, Jansen M, Akabas MH, and Goldman ID (2008) The proton-coupled folate transporter: impact on pemetrexed transport and on antifolates activities compared with the reduced folate carrier. *Mol Pharmacol* **74:** 854-862.

Zeng H, Chen ZS, Belinsky MG, Rea PA, and Kruh GD (2001) Transport of methotrexate (MTX) and folates by multidrug resistance protein (MRP) 3 and MRP1: effect of polyglutamylation on MTX transport. *Cancer Res* **61:** 7225-7232.

Zheng W, and Zhao Q (2002) Establishment and characterization of an immortalized Z310 choroidal epithelial cell line from murine choroid plexus. *Brain Res* **958:** 371–380.

Molecular Pharmacology Fast Forward. Published on July 7, 2011 as DOI: 10.1124/mol.111.072421
This article has not been copyedited and formatted. The final version may differ from this version.

Footnotes

a) This work was supported by the Deutsche Forschungsgemeinschaft [Grant HO-2103/2-1].

c) Person to receive reprint requests: Sandra Halwachs, Institute of Pharmacology, Pharmacy and Toxicology, Faculty of Veterinary Medicine, An den Tierkliniken 15, University of Leipzig, 04103 Leipzig, Germany; Tel.: +49 (0) 341-9738142, FAX +49 (0) 341-9738149; E-mail: halwachs@vetmed.uni-leipzig.de

Molecular Pharmacology Fast Forward. Published on July 7, 2011 as DOI: 10.1124/mol.111.072421
This article has not been copyedited and formatted. The final version may differ from this version.

Legends for figures

Fig. 1. (A) Expression of organic anion transporters in Z310 cells and rat choroid plexus. Total RNA was isolated and used for RT-PCR analysis as described in Material and Methods. Sizes of the expected PCR products and the specific primers that were used are listed in Table 1S. Arrowheads indicate weak bands obtained for Oat1 in Z310 cells and Mrp4 as well as Mrp6 in choroid plexus tissue. RT-PCR of G3PDH served as a positive control. (B) Western blot analysis of MTX transporters in Z310 cells. Equal protein amounts (50 µg) were separated on a SDS polyacrylamide gel and selective MTX carrier were detected using specific antibodies as delineated in Material and Methods. Specific protein bands were obtained for Oat3 (130 kDa), Rfc1 (56 kDa), Bcrp (72 kDa) and Mrp1 (190 kDa). ß-actin was used as a loading control. The Western blot shown is representative of at least 2 independent experiments.

Fig. 2. Subcellular localization of Rfc1, BCRP and Mrp1 and detection of ZO-1 in Z310 cells. Cells were grown on permeable Transwell filter inserts. (A and B) Polarized Z310 cell monolayers were fixed and stained for Rfc1 (*green*) and Bcrp (*red*). (C) Polarized cells were fixed and stained Mrp1 (*red*) and ZO-1 (*green*). Generally, cell nuclei (*blue*) were visualized using DAPI. (A-C) Optical XY sectioning was performed by confocal laser scanning microscopy. (A and C) White arrowheads indicate positions of the corresponding XZ- or YZ-section. Rfc1 as well as Bcrp were predominantly localized to the apical surface of Z310 cells (A and B). Colocalization of Rfc1 and Bcrp results in yellow/orange. (C) Mrp1 was predominantly found at the basolateral membrane and partly colocalize with ZO-1 resulting in yellow/orange staining. Control incubations included omission of primary antibody. Representative cells are shown from two independent experiments. Bars, 5 µm

Molecular Pharmacology Fast Forward. Published on July 7, 2011 as DOI: 10.1124/mol.111.072421
This article has not been copyedited and formatted. The final version may differ from this version.

Fig. 3. Rfc1 activity in Z310 cells as measured as the sodium-dependent and MTHF-sensitive uptake of MTX. (A) Cells were harvested and the culture medium was replaced by aCSF (129 mM Na^+) or sodium-free Choline-aCSF and 5 µM MTX containing 2 x 10^5 dpm [^{3}H] MTX. (B) Cells were incubated in aCSF with MTX (5 µM) in the absence or presence of 0.13 mM or 0.25 mM MTHF. Generally, uptake was stopped at the indicated time points by centrifugation of aliquots through a silicon oil cushion and the incorporated radioactivity was measured by liquid scintillation counting. Rfc1 activity was defined as the sodium-dependent uptake of MTX (5 µM) over 5 min and expressed in pmol per mg protein. The data represent the mean ± SEM of at least two different measurements with n ≥ 5. ** $p < 0.01$, *** $p < 0.001$.

Fig. 4. Effect of Mrp-inhibitor MK571 or BCRP-inhibitor Ko143 on MTX accumulation in Z310 cells. (A) Cells were incubated with 5 µM [^{3}H] MTX in the absence or presence of 50 and 100 µM MK571 or 1 and 5 µM Ko143 (B) for 20 min. Generally, MTX accumulation in Z310 cells was measured in aCSF at the indicated time points as delineated in the legend for Fig. 3 and expressed in pmol per mg protein. The data represent the mean ± SEM of at least two different measurements with n ≥ 5. * $p < 0.05$, ** $p < 0.01$, *** $p < 0.001$.

Fig. 5. Effect of AEDs on Rfc1-mediated MTX uptake in choroid plexus epithelial cells. Z310 cells were treated with therapeutic and 10X therapeutic concentrations of PB (A), CBZ (B), or gabapentin (C) for 48 h. Generally, cellular MTX accumulation in the presence or absence of extracellular sodium was measured in aCSF at the indicated time points as delineated in the legend for Fig. 3. Rfc1 activity was defined as the sodium-dependent uptake of MTX (5 µM) over 2.5 min and expressed in pmol per mg protein. The data represent the mean ± SEM of at least two different measurements in which quadruplicates were obtained. ** $p < 0.01$, *** $p < 0.001$.

Molecular Pharmacology Fast Forward. Published on July 7, 2011 as DOI: 10.1124/mol.111.072421
This article has not been copyedited and formatted. The final version may differ from this version.

Fig. 6. Impact of PB on Rfc1 expression. (A) Z310 cells were pre-treated with 43 or 430 µM PB for 48 h. Rfc1 transcript levels were analysed by quantitative RT-PCR using 1 µg of total RNA and rat gene specific Rfc1 primers and probes as described in Material and Methods. Relative Rfc1 mRNA levels were expressed as the percentage of the Rfc1 gene expression comparatively to the control level. ß-actin was used as an internal standard. The data represent the mean ± SEM of three different measurements in which quadruplicates were obtained. (B) Z310 cells were incubated with 43 or 430 µM PB for 48 h and Rfc1 protein levels were assessed by Western blot. Equal protein amounts (50 µg) were separated on a SDS/10% polyacrylamide gel and specific protein bands of ~ 56 kDa for Rfc1 (→) were obtained using specific anti-SLC19A1 antibody. ß-actin was used as a loading control and is apparent at ~ 45 kDa (→). The Western blot shown is representative of two independent experiments. Densitometric analysis of Rfc1 immunoreactivity in consideration of the background value is shown. Results are expressed as means ± SD for duplicate determinations. * $p < 0.05$.

Figure 1

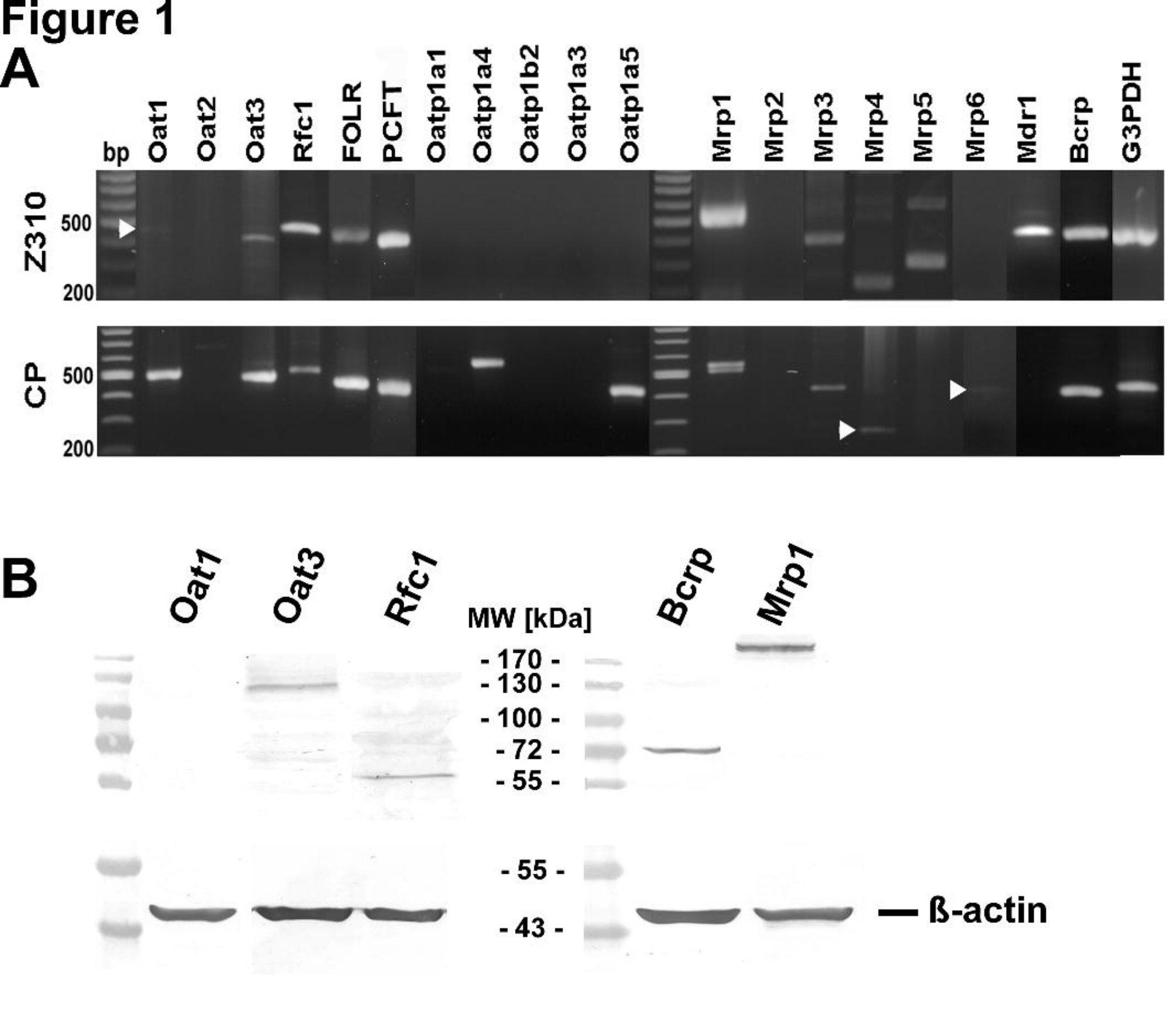
A
bp
Oat1
Oat2
Oat3
Rfc1
FOLR
PCFT
Oatp1a1
Oatp1a4
Oatp1b2
Oatp1a3
Oatp1a5
Mrp1
Mrp2
Mrp3
Mrp4
Mrp5
Mrp6
Mdr1
Bcrp
G3PDH
Z310
500
200
CP
500
200
B
Oat1
Oat3
Rfc1
MW [kDa]
Bcrp
Mrp1
- 170 -
- 130 -
- 100 -
- 72 -
- 55 -
- 55 -
- 43 -
ß-actin

Figure 2A

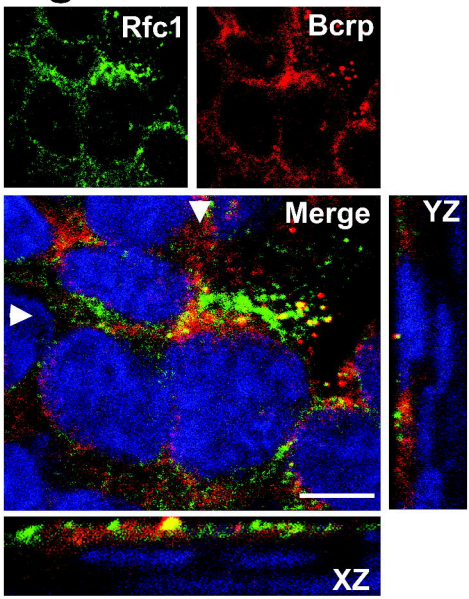
Rfc1
Bcrp
Merge
YZ
XZ

B

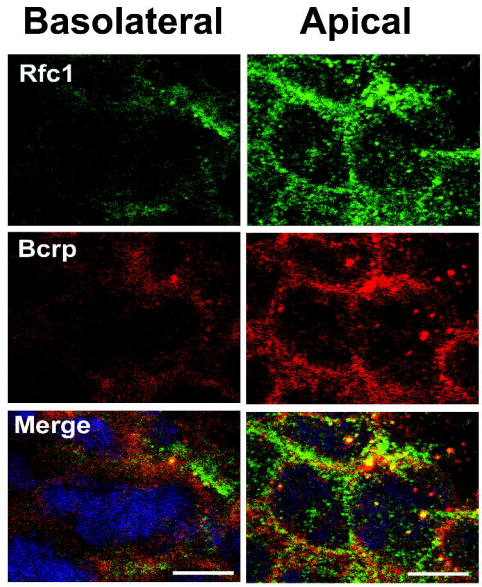
Basolateral
Apical
Rfc1
Bcrp
Merge

C

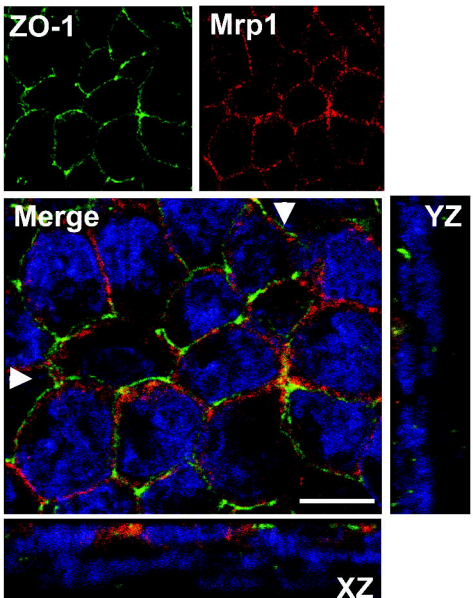
ZO-1
Mrp1
Merge
YZ
XZ

Figure 3

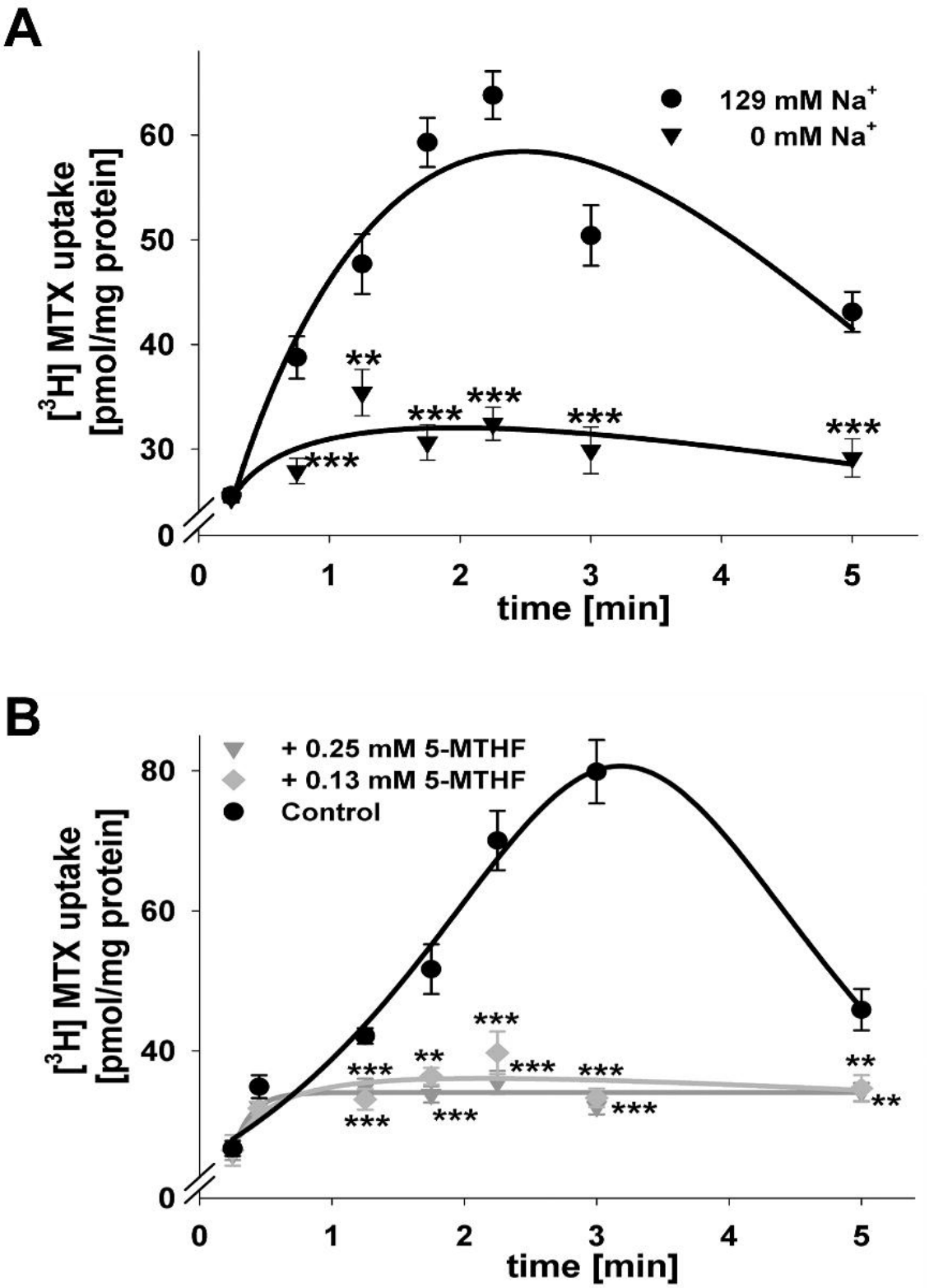
A
[3H] MTX uptake [pmol/mg protein]
129 mM Na+
0 mM Na+
time [min]
B
+ 0.25 mM 5-MTHF
+ 0.13 mM 5-MTHF
Control
[3H] MTX uptake [pmol/mg protein]
time [min]

Figure 4

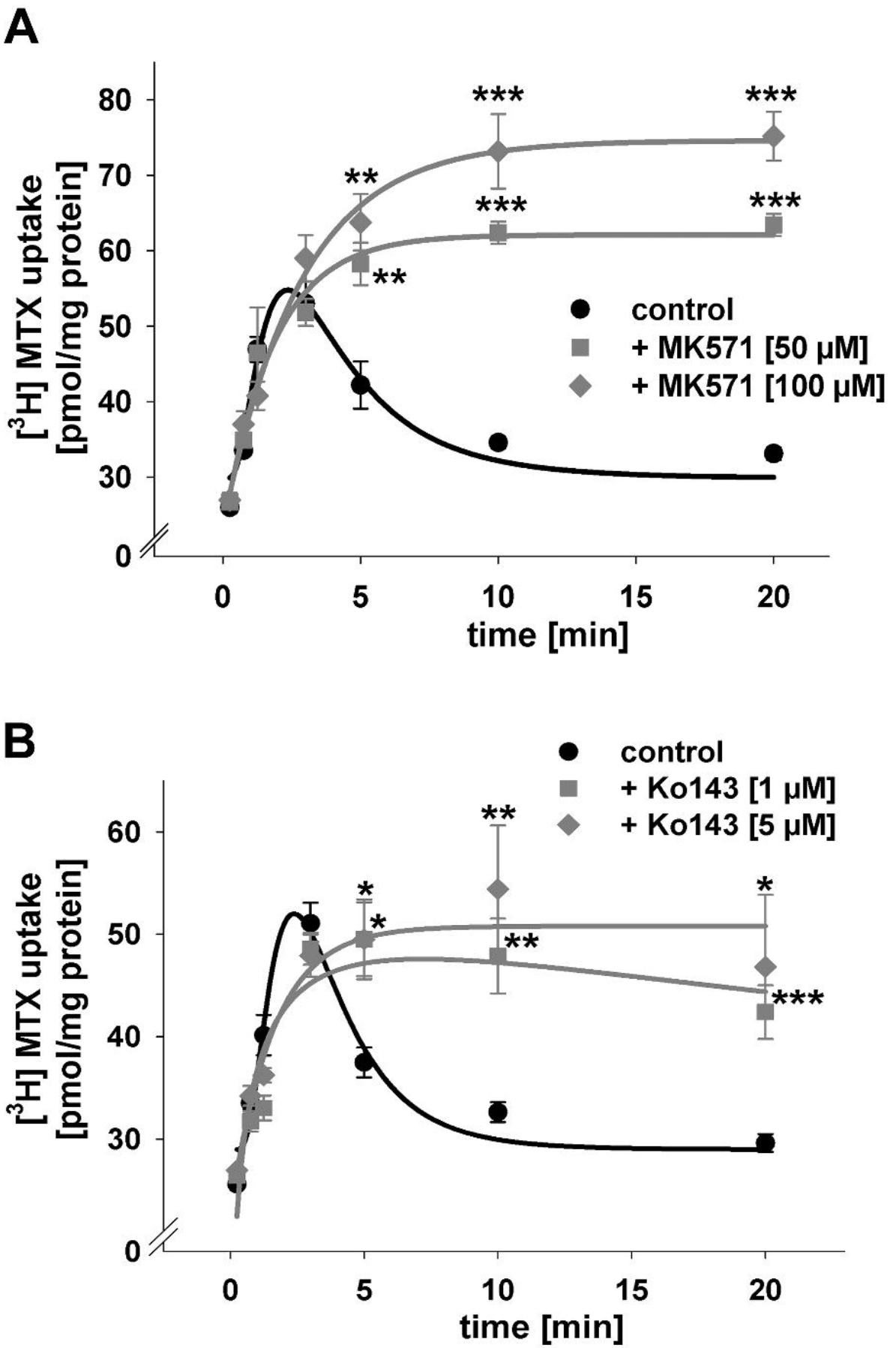
A
[3H] MTX uptake [pmol/mg protein]
80
70
60
50
40
30
0
0
5
10
15
20
time [min]
control
+ MK571 [50 µM]
+ MK571 [100 µM]
**
***
***
**
***
***
B
[3H] MTX uptake [pmol/mg protein]
60
50
40
30
0
0
5
10
15
20
time [min]
control
+ Ko143 [1 µM]
+ Ko143 [5 µM]
*
*
**
**
*
***

Figure 5

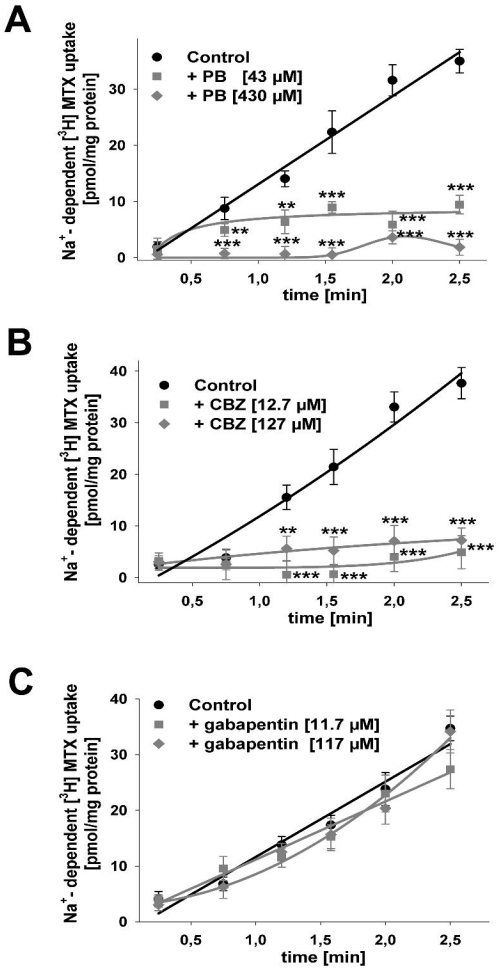
A
Control
+ PB [43 µM]
+ PB [430 µM]
Na+ - dependent [3H] MTX uptake [pmol/mg protein]
time [min]
B
Control
+ CBZ [12.7 µM]
+ CBZ [127 µM]
Na+ - dependent [3H] MTX uptake [pmol/mg protein]
time [min]
C
Control
+ gabapentin [11.7 µM]
+ gabapentin [117 µM]
Na+ - dependent [3H] MTX uptake [pmol/mg protein]
time [min]

Figure 6

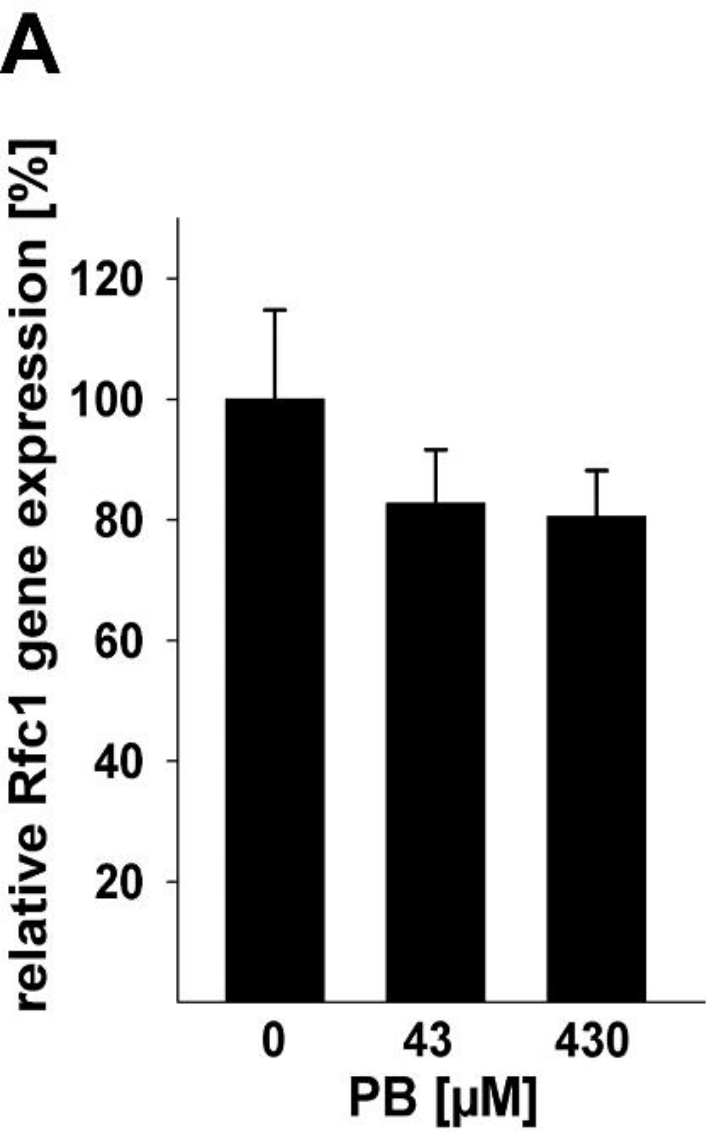
A
relative Rfc1 gene expression [%]
120
100
80
60
40
20
0
43
430
PB [µM]

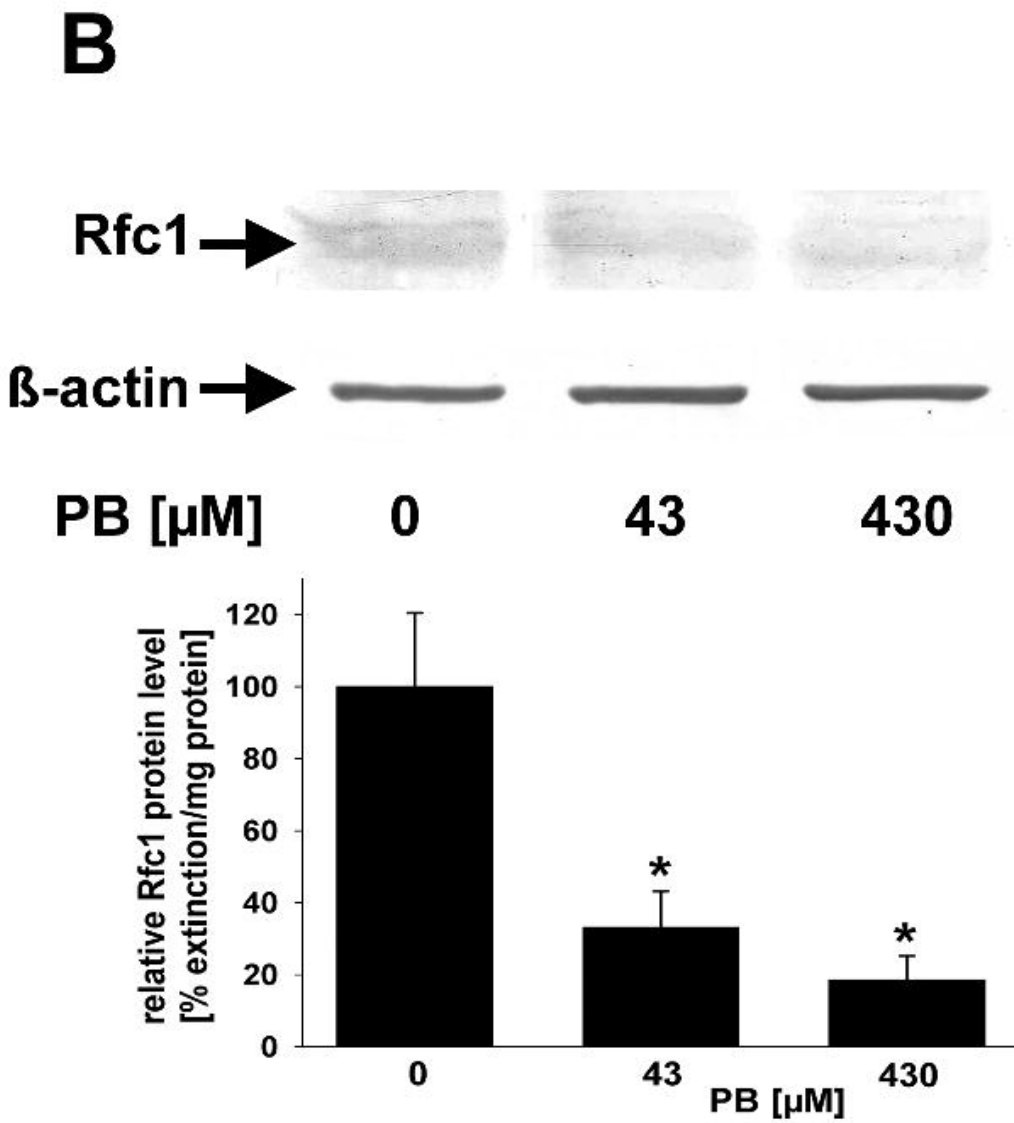
B
Rfc1
ß-actin
PB [µM]
0
43
430
relative Rfc1 protein level
[% extinction/mg protein]
120
100
80
60
40
20
0
*
*
0
43
430
PB [µM]